Supporting Information

Upadhyay et al. 10.1073/pnas.1221206110

SI Materials and Methods

Diet. For obesity induction, we chose a rodent diet to mimic the Western diet (rich in fat and carbohydrate) that is linked to risk of cardiovascular diseases in humans. The diet consisted of Teklad TD.88137 together with 60% fructose/water (wt/vol) available ad libitum (Table S2*A*). The Teklad TD.88137 is often referred to as the Western diet and has been used in mouse models of diet-induced obesity, including in studies of brown fat function and hepatic steatosis (1–3). This diet is richer in fat and lower in carbohydrate than the chow diet (Tables S2 and S3). We added 60% fructose/water (wt/vol) to the obesity diet because the increased consumption of high-fructose corn syrup is linked to the development of metabolic syndrome, hyperuricemia, insulin resistance, hypertension, and renal disease (4–6). For the normal chow diet, we used the Teklad 7001 4% fat mouse diet (Table S3). Water was available ad libitum. Table S3 compares the chow and obesity diets used in this study with those previously used on $Kv1.3^{-/-}$ mice (7–9). Tables S5–S7 show the calorie consumption from solid food and fluid in control and treated mice given the obesity diet. Fructose consumption was calculated as

$$\text{milliliters of fructose/water consumed} \times \text{fructose concentration (wt/vol)} \times 4 = \text{kcal}.$$

ShK-186 Synthesis, Formulation, and Characteristics. ShK-186 was manufactured using an Fmoc-tBu solid-phase strategy as described (10). The peptide was formulated at 0.5–25 mg/mL in 10 mM sodium phosphate, 0.8% NaCl, 0.05% polysorbate 20 (pH 6) (10). Animals were administered either ShK-186 or vehicle (P6N = PBS containing 0.05% Tween 20) by s.c. injection. ShK-186 has durable in vivo pharmacological action in rodents and nonhuman primates (10), which allowed us to administer ShK-186 by s.c. injection every other day. The doses we used were allometrically determined from doses used in rat models of autoimmune diseases, though there was no way to know if ShK-186 would be as effective in preventing obesity as it is in treating autoimmune disease. In rats, ShK-186 100 μg/kg is effective in treating disease in models of multiple sclerosis and rheumatoid arthritis (10–12). Allometrically, this dose is equivalent to ∼200 μg/kg in mice (exponent used 0.75). We chose one higher dose (500 μg/kg) and one lower dose (20 μg/kg) for our study.

Quantitative RT-PCR and Analysis. cDNA synthesis was done using the iScript cDNA Synthesis Kit (Bio-Rad). The quantitative PCR (qPCR) reaction was done with the iQ SYBR Green Supermix (Bio-Rad). qPCR was performed using the Chromo4 Real-Time PCR Detection System (Bio-Rad). Expression is reported relative to 18S RNA. The data were analyzed by

$$[2e(40 - \text{Ct})\text{Exp} - \text{gene}/2e(40 - \text{Ct})18\text{S}] \times 10^6.$$

Body Temperature. Body temperature (skin) was measured on 2 d during the study at 6:00 AM, 12 noon, and 6:00 PM using an infrared thermometer (Kintrex IRT-0412).

Comprehensive Lab Monitoring System Measurement of Feeding, Drinking, Respiratory Exchange Ratio, and Energy Expenditure. We used negative-flow Comprehensive Lab Monitoring System (CLAMS) hardware system cages (Columbus Instruments) for recording metabolic parameters. Oxymax software (Columbus Instruments) was used to measure heat, respiratory exchange ratio (RER), and related calculations. Mice from week 10 of the prevention trial were housed individually in metabolic cages and allowed to acclimate for 4 d with 12-h light/dark cycles. Feeding, drinking, RER, and energy expenditure (EE) were measured over the next 36 h. The mice received their scheduled dose of ShK-186 or vehicle before the recording period, usually at 5:30 PM. The study was designed to avoid disturbing the mice once recording started. We did not want to remove mice from the CLAM cages to administer s.c. injections of vehicle or ShK-186, because such an intervention could affect the experiment. We exploited the durable pharmacological action of ShK-186 by administering the drug every other day, and measuring metabolic data over 36 h after the scheduled drug administration. The Oxymax calculation of energy expenditure was based on the equation

$$\text{heat} = \text{calorific value} \ (3.815 + 1.232 \times \text{RER}) \times \text{VO}_2.$$

The calorie expenditure in control and treated mice fed an obesity diet is shown in Table S4.

Immunostaining. Formalin-fixed paraffin-embedded mouse tissues mounted on the glass slides were used for immunohistochemical staining. Sections were dewaxed with xylene (5 min, three times) and rehydrated through an alcohol gradient (100–30%). Before staining with the primary antibody, sections were steam-treated with low-pH antigen retrieval solution (Vector Laboratories H3300) for 20 min to retrieve antigens masked by paraffin embedding. Endogenous peroxidase activity was blocked by 1.5% (wt/vol) hydrogen peroxide solution in PBS for 20 min. After blocking with 5% (wt/vol) goat serum, 5% (wt/vol) BSA, and 0.1% sodium azide in PBS, sections were incubated with primary antibody overnight at 4 °C. We used a rabbit polyclonal anti-Kv1.3 antibody (a gift from Hans Günther-Knaus, University of Innsbruck, Innsbruck, Austria) and rabbit polyclonal anti–uncoupling protein 1 (UCP1; Abcam ab23841). Bound primary Ab was detected with biotinylated goat anti-rabbit Ab followed by an HRP-conjugated avidin complex using a Vectastain Elite ABC Kit (Vector Laboratories). Peroxidase activity was visualized with 3,3′-diaminobenzidine (DAB) using a DAB substrate kit for peroxidase (Vector Laboratories; SK-4100). Sections were counterstained with hematoxylin (Fisher Scientific) and bluing solution, dehydrated through the alcohol gradient and xylene washes, and mounted with Permount (Fisher Scientific).

Thyroid Hormone. Blood was collected in heparin-coated tubes. Plasma was separated, and shipped to Ani Lytics, Inc., for measurement of T3 and T4 hormones by RIA.

Leptin. Leptin was measured using ELISA (MMHMAG-44K; Millipore).

Blood Sugar. Blood was obtained by tail prick and blood glucose determined using the AccuChek Compact Plus glucometer (Roche Diagnostics). HbA1c measurement was performed at the Comparative Pathology Laboratory at University of California, Davis, using ELISA.

Intraperitoneal Glucose Tolerance Test. The i.p. glucose tolerance test was performed on the off-day when drug or vehicle was not administered. Mice were fasted for 8 h, and then administered 2 g/kg glucose by i.p. injection. Blood glucose levels were measured at various time points using the AccuChek Compact Plus glucometer. Blood was collected in heparin-coated capillary tubes

at time 0 and 15 min for measurement of blood insulin levels using an ELISA (ALPCO).

Insulin Tolerance Test. The insulin tolerance test was performed on the on-day of therapy. After an overnight fast, mice received their scheduled injection of vehicle or ShK-186, followed 1 h later by an s.c. injection of 0.75 U/kg normal insulin (HumulinR; Lilly). Blood glucose was measured at various times thereafter using the AccuChek Compact Plus glucometer.

Locomotor Activity. Male mice from the prevention trial were examined >8 wk after the start of the cafeteria diet and therapy (vehicle or 500 μg/kg ShK-186). Animals were placed in individual cages with passive (pyroelectric) infrared sensors (PU-2201; EK Japan) and habituated under conditions of 12-h light/dark cycles for 3 d before recording data; they continued to receive the cafeteria diet and received their scheduled doses of ShK-186 or vehicle. Activity data were collected using the VitalView data acquisition system (Mini-Mitter) with a sampling interval of 5 min. The actograms were acquired using Actiview Biological Rhythm Analysis software (Mini-Mitter) and analyzed using Locklabs software (Actimetrics).

PET/CT Imaging. This method has been widely used in mice and humans to assess the metabolic activity of brown adipose tissue (BAT) (13). Following an overnight fast, mice were injected with vehicle or ShK-186, and 30 min later they received i.v. administration of 2-deoxy-2-(^{18}F)-fluoro-D-glucose (^{18}F-FDG; 2.23 ± 0.68 mBq) under isoflurane (2%) anesthesia. One hour later they were placed in the supine position in a mouse holder and anesthetized with 2% isoflurane for 30 min-long PET imaging. All mice had a CT scan after the PET scan for attenuation-correction and anatomical delineation of PET images. PET images were spatially transformed to match the reconstructed CT images as described previously (13). All images were analyzed using PMOD Software (PMOD Technologies) and Inveon Research Workplace (IRW) software (Siemens Medical Solutions). A Sigma Delta anesthetic vaporizer (DRE Medical Equipment) was used to induce and maintain anesthesia during intravascular injections and PET/CT acquisitions. Radioactivity was counted using CRC-15R dose calibrator (Capintec). The ^{18}F-fluorodeoxyglucose (^{18}F-FDG) was purchased from PETNET Solutions. Isoflurane was purchased from Clipper Distributing Company. The magnitude of BAT ^{18}F-FDG activation was expressed as standard uptake values, defined as the average ^{18}F-FDG activity in each volume of interest (VOI; in kBq/mL) divided by the injected dose (in mBq) times the body weight of each animal (in kilograms). For quantitative analysis, VOIs were drawn on PET images for interscapular BAT and on CT images for white adipose tissue (WAT) and skeletal muscle (biceps brachii) using the program PMOD. As described previously, the VOIs were delineated visually by contouring the ^{18}F-FDG activity that was clearly above normal background activity (2). Statistical analysis was by paired, two-tailed Student *t* test with significance at $P < 0.05$.

CT Scan to Assess WAT, Fatty Liver, and Lean Tissue Volume. This method has been widely used in mice and humans to assess WAT volume and lean body volume (14, 15). Mice were studied at week 10 of the study. All CT acquisitions were performed on anesthetized mice (2% isoflurane). Each animal underwent a high-resolution CT scan with an Inveon Multimodality CT scanner. The CT scan was performed at a one-bed position with detector-source rotating 360° around the animal with projections acquired every 1° (360 angles). CT images were reconstructed with a cone-beam algorithm (bilinear interpolation; Shepp-Logan filter) into 480 × 480 × 1,024 with the Inveon (Siemens Medical Solutions) preclinical CT scanner. Segmentation and measurement of WAT and whole-body volumes were done using PMOD as described previously (14, 15). Assessment of liver fat content was done by CT scan on the basis of previously established criteria (16). Regions of interest (ROIs) were placed on 10 areas of the liver and 10 areas of the spleen at different depths from the liver and the splenic capsule to construct the VOIs. Care was taken not to include major portal, arterial, and venous vessels. For each VOI, the attenuation measured in Hounsfield units (HU) was recorded. The HU scale is a linear transformation of the original linear attenuation coefficient measurement into one in which the radiodensity of distilled water at standard pressure and temperature is defined as zero HU, and the radiodensity of air is defined as −1,000 HU. In a voxel with average linear attenuation coefficient μ_X, the corresponding HU value is therefore given by

$$\mathrm{HU} = 1,000 \times \frac{\mu_x - \mu_{\mathrm{Water}}}{\mu_{\mathrm{Water}}}.$$

In this equation, μ_{water} is the linear attenuation coefficient of water. Thus, a change of 1 HU represents a change of 0.1% of the attenuation coefficient of water. The mean liver and spleen attenuations were obtained by PMOD, and the ratio of mean liver attenuation to spleen attenuation (L/S) was determined. L/S is inversely related to hepatic fat content such that the lower the L/S, the greater the amount of fat in the liver.

Blood Lipid Profile. Blood was collected by cardiac puncture using heparin as anticoagulant. Samples were shipped to the Comparative Pathology Laboratory, School of Veterinary Medicine, University of California, Davis, for measurement of cholesterol, LDL, HDL, triglycerides, and free fatty acids. The assay was done with the Roche Diagnostics COBAS INTEGRA 400 Plus system.

Histopathological Analysis of Heart, BAT, Liver, WAT, and Skeletal Muscle. Tissues were collected from mice at the end of a prevention trial. Interscapular BAT, visceral WAT, and the liver were removed, formalin-fixed, and shipped to the Comparative Pathology Laboratory, University of California, Davis, for pathological analysis. Fat accumulation and histologic changes were assessed by H&E and confirmed by Oil Red O staining on routinely processed tissue sections.

Metabolite Profile Measurement and Analysis in Liver and Visceral WAT. Interscapular BAT (six controls and eight treated), liver (eight controls, eight treated), and visceral WAT (seven controls and seven treated) were collected 10 wk after the initiation of the obesity diet and therapy. Samples were stored at −80 °C until extracted and prepared for analysis using Metabolon's standard solvent extraction method. Extracted samples were split into equal parts for analysis on the three independent platforms: ultrahigh-performance liquid chromatography/tandem mass spectrometry (UHPLC/MS/MS) optimized for basic species, UHPLC/MS/MS optimized for acidic species, and gas chromatography/mass spectrometry (GC/MS). Several technical replicate samples created from a homogeneous pool containing a small amount of all study samples (client matrix samples) were used as comparators on the platforms. Instrument variability was determined by calculating the median relative SD (RSD) for the internal standards that were added to each sample before injection into the mass spectrometers. Overall process variability was determined by calculating the median RSD for all endogenous metabolites (i.e., noninstrument standards) present in 100% of the client matrix samples. Following log transformation and imputation with minimum observed values for each compound, Welch's two-sample *t* tests were used to identify metabolites that differed significantly between experimental groups. Metabolites that achieved statistical significance ($P \leq 0.05$), as well as those approaching significance ($0.05 < P < 0.1$), are discussed in *Results*. The q-values for metabolite analysis were determined to assess

false positives. The q-value describes the false discovery rate; a low q-value ($q < 0.10$) is an indication of high confidence in a result.

Hanging Wire Test. Four limb-hanging test experiments were done as described earlier (17, 18). Briefly, animals were allowed to hang from a wire mesh placed ~30 cm above the bedding, and the hanging time was recorded.

Western Blot. Livers and interscapular BAT were obtained from mice 10 wk after start of the study. Mice were on either a chow diet with water or an obesity-inducing diet rich in fat and fructose. Fifty micrograms of protein from liver tissue or interscpaular BAT lysate was loaded into each well for Western blot analysis. Rabbit polyclonal anti-Kv1.3 antibody (1:500; a gift from Hans Günther-Knaus, University of Innsbruck, Innsbruck, Austria) was used as primary antibody, and HRP-conjugated goat anti-rabbit (1:2,000) was used as secondary antibody. For actin, we used mouse monoclonal (mAbcam 8226). Scans were calibrated and measured using ImageJ software, developed by the National Institutes of Health. Optical density measurements of the 60-kDa and 80-kDa Kv1.3 bands were made separately, and these values were normalized to total actin per lane. The quantitation of the two Kv1.3 bands in BAT and livers of two mice on the chow diet and two mice on the obesity-inducing diet is shown in Tables S8 and S9.

Two-Dimensional Differential Gel Electrophoresis Coupled with Tandem Mass Spectrometry. Liver samples from vehicle and ShK-186 (500 μg/kg)-treated mice on the obesity diet were weighed, homogenized in sample buffer [7 M urea, 2 M thiourea, 4% (wt/vol) CHAPS, and 40 mM DTT; 10 mg liver per milliliter of sample buffer], and then incubated on ice for 30 min. Homogenates were centrifuged at 16,000 × g for 15 min at 4 °C, supernatants collected, and protein quantified with a Bradford protein assay. Samples from three vehicle-treated mice and three ShK-186–treated mice were pooled and labeled with either Cy3 or Cy5 fluorescent dyes. The internal standard was labeled with Cy2 fluorescent dye. Isoelectric focusing was done using an Ettan IPGphor 3. Strips were equilibrated, and proteins reduced and alkylated before PAGE (GE Healthcare) on 6–18% gradient gels (Jule Inc.) overlaid with 1% (wt/vol) low-melting agarose. Gels were run at 25 °C in an Ettan DALT II system. A Typhoon FLA 9500 (GE Healthcare) was used to image Cy2, Cy3, and Cy5 components of each gel. DeCyder 6.5 was used for spot quantification and statistical analysis. Spots with $P < 0.05$ and abundance ratios >+1.5 or <−1.5 were retained for evaluation. The 2D gel was stained (19) and in-gel digestion was performed (20). Samples were subsequently desalted using ZipTips (Millipore) and 1 μL spotted directly onto a MALDI plate using the dried-droplet method. Mass spectrometry was performed on an AB SCIEX TOF/TOF 5800 system. Spectra from MALDI-TOF were acquired in positive ion reflector mode over a mass range of 0.8–4 kDa. MS/MS spectra were acquired in 1-kV positive mode. A mass accuracy tolerance of 30 ppm for precursor and 0.3 Da for fragments were used for all tryptic mass searches of *Mus musculus* proteins using the Paragon algorithm (ProteinPilot v3.0; AB SCIEX). The expression of ~125 proteins was significantly altered in the livers of ShK-186–treated mice. We have analyzed two of these—carbamoyl phosphate synthase 1 and S-adenosylhomocysteinase—that corroborate the metabolomics and the qPCR data.

Statistical Analysis. We used the pairwise Student t test, repeated-measures two-way ANOVA followed by post hoc Bonferroni correction, one-way ANOVA with post hoc Bonferroni correction, and Welch's t test as referred to in the figure legends.

1. Meek TH, Eisenmann JC, Garland TR, Jr. (2010) Western diet increases wheel running in mice selectively bred for high voluntary wheel running. *Int J Obes (Lond)* 34(6):960–969.
2. Xu X, et al. (2011) Exercise ameliorates high-fat diet-induced metabolic and vascular dysfunction, and increases adipocyte progenitor cell population in brown adipose tissue. *Am J Physiol Regul Integr Comp Physiol* 300(5):R1115–R1125.
3. Alkhouri N, et al. (2010) Adipocyte apoptosis, a link between obesity, insulin resistance, and hepatic steatosis. *J Biol Chem* 285(5):3428–3438.
4. Johnson RJ, Sanchez-Lozada LG, Nakagawa T (2010) The effect of fructose on renal biology and disease. *J Am Soc Nephrol* 21(12):2036–2039.
5. Sun SZ, Empie MW (2012) Fructose metabolism in humans—what isotopic tracer studies tell us. *Nutr Metab (Lond)* 9(1):89.
6. Lustig RH (2010) Fructose: Metabolic, hedonic, and societal parallels with ethanol. *J Am Diet Assoc* 110(9):1307–1321.
7. Tucker K, Overton JM, Fadool DA (2008) Kv1.3 gene-targeted deletion alters longevity and reduces adiposity by increasing locomotion and metabolism in melanocortin-4 receptor-null mice. *Int J Obes (Lond)* 32(8):1222–1232.
8. Tucker KR, Godbey SJ, Thiebaud N, Fadool DA (2012) Olfactory ability and object memory in three mouse models of varying body weight, metabolic hormones, and adiposity. *Physiol Behav* 107(3):424–432.
9. Xu J, et al. (2003) The voltage-gated potassium channel Kv1.3 regulates energy homeostasis and body weight. *Hum Mol Genet* 12(5):551–559.
10. Tarcha EJ, et al. (2012) Durable pharmacological responses from the peptide ShK-186, a specific Kv1.3 channel inhibitor that suppresses T cell mediators of autoimmune disease. *J Pharmacol Exp Ther* 342(3):642–653.
11. Beeton C, et al. (2006) Kv1.3 channels are a therapeutic target for T cell-mediated autoimmune diseases. *Proc Natl Acad Sci USA* 103(46):17414–17419.
12. Beeton C, et al. (2005) Targeting effector memory T cells with a selective peptide inhibitor of Kv1.3 channels for therapy of autoimmune diseases. *Mol Pharmacol* 67(4):1369–1381.
13. Mirbolooki MR, Constantinescu CC, Pan ML, Mukherjee J (2011) Quantitative assessment of brown adipose tissue metabolic activity and volume using 18F-FDG PET/CT and β3-adrenergic receptor activation. *EJNMMI Res* 1(1):30.
14. Sasser TA, et al. (2012) Segmentation and measurement of fat volumes in murine obesity models using X-ray computed tomography. *J Vis Exp* 62:e3680, 10.3791/3680.
15. Lubura M, et al. (2012) Non-invasive quantification of white and brown adipose tissues and liver fat content by computed tomography in mice. *PLoS ONE* 7(5):e37026.
16. Ma X, et al. (2009) Imaging-based quantification of hepatic fat: Methods and clinical applications. *Radiographics* 29(5):1253–1277.
17. Shakkottai VG, et al. (2004) Enhanced neuronal excitability in the absence of neurodegeneration induces cerebellar ataxia. *J Clin Invest* 113(4):582–590.
18. Klein SM, et al. (2012) Noninvasive in vivo assessment of muscle impairment in the mdx mouse model—a comparison of two common wire hanging methods with two different results. *J Neurosci Methods* 203(2):292–297.
19. Wang X, Li X, Li Y (2007) A modified Coomassie Brilliant Blue staining method at nanogram sensitivity compatible with proteomic analysis. *Biotechnol Lett* 29(10):1599–1603.
20. Shevchenko A, Wilm M, Vorm O, Mann M (1996) Mass spectrometric sequencing of proteins silver-stained polyacrylamide gels. *Anal Chem* 68(5):850–858.

A

Group	Blood Cholesterol (mg/dl)	Blood LDL (mg/dl)	HDL (mg/dl)	Triglyceride (mg/dl)	Free Fatty Acid mEq/L	Leptin (ng/ml)	Uric Acid	Liver histology
Obesity Diet								
Vehicle	288.9 ± 9.6	94.2 ± 6.3	228.9 ± 6.7	50.2 ± 6.6	2.9 ± 0.3	57.0 ± 10.0	2.3 ± 0.4	Fatty liver
ShK-186 500µg	234.5 ± 13.4**	72.5 ± 6.5**	178.9 ± 15.1*	54.3 ± 6.5	3.1 ± 0.3	21.5 ± 3.4*	1.3 ± 0.3	Reduced fatty liver
ShK-186 20 µg	225.2 ± 13.3**	62.2 ± 9.2**	189 ± 8.9*	47.3 ± 9.4	2.1 ± 0.3	13.9 ± 5.9**	2.8 ± 0.3	Not done
Chow Diet								
Vehicle	144.3 ± 24	12.0 ± 2.0	153.1 ± 26.3	88.5 ± 16.3	1.5 ± 0.3	12.8 ± 6.7	3.4 ± 0.7	No fatty liver
ShK-186 500 µg	114 ± 17.3*	7.2 ± 1.3*	115.0 ± 17.8*	52.8 ± 10.3*	1.4 ± 0.2	6.7 ± 1.4	2.1 ± 0.4	No fatty liver

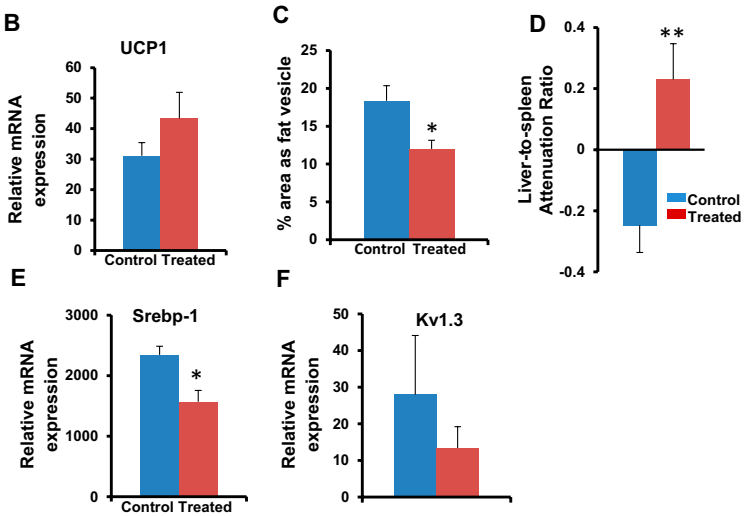

Fig. S1. Effects of ShK-186 on dyslipidemia and fatty liver. (*A*) Blood levels of cholesterol, triglyceride, free fatty acids, HDL and LDL and state of fatty liver in control and treated mice fed either obesity or chow diet; $n = 10–11$ (each group) for mice on obesity diet, $n = 7$ (each group) for mice on chow diet. The significant decrease in cholesterol in mice on chow diet has also been seen in rats and monkeys on normal diet. (*B*) mRNA levels (mean ± SEM) of UCP1 in visceral WAT of vehicle and ShK-186–treated animals. (*C*) Quantitation of fat accumulation in livers of control and treated mice from histological sections stained with Oil Red. (*D*) Quantification of fat accumulation in the liver measured by CT scan showed a higher liver-to-spleen attenuation ratio in treated mice, which indicates decreased fat accumulation ($P = 0.01$). (*E*) Sterol regulatory-element binding protein 1 and (*F*) Kv1.3 mRNA levels in the liver of control and treated mice. Color code for *B*–*F*: blue, vehicle-control; brown, ShK-186–treated. Student *t* test was performed to determine significance of differences between means. Student *t* test; $*P < 0.05$, $**P < 0.01$.

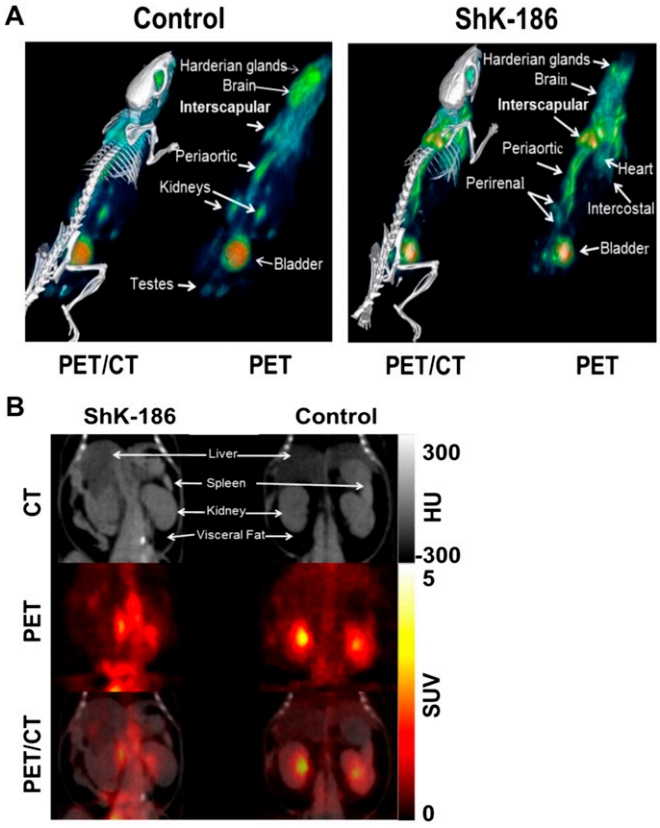

Fig. S2. PET/CT scans of control and treated mice. (*A*) PET and PET/CT 3D images showing ^{18}F-FDG uptake into different tissues in a control mouse (*Left*) and a ShK-186–treated mouse (*Right*). (*B*) CT images (*Top*) in HU shows darkened areas of visceral fat. PET (*Middle*) and PET/CT images (*Bottom*) show that visceral fat does not take up any ^{18}F-FDG in control or treated mice.

A

	BAT Fold Change	BAT p value	Liver Fold Change	Liver p value	WAT Fold Change	WAT p value
Medium Chain Fatty Acid						
caproate (6:0)	0.85	0.5888	0.78	0.0452	0.84	0.4252
caprylate (8:0)	1.18	0.2633	0.93	0.6856	1.97	0.429
caprate (10:0)	1.25	0.116			1.03	0.8544
undecanoate (11:0)	1.1	0.1554			0.79	0.2453
laurate (12:0)	1	0.8513	1.17	0.0033	1	0.7961
pelargonate (9:0)			1.13	0.1865	1.18	0.3486
Long Chain Fatty Acid						
myristate (14:0)	1.02	0.8982	1.09	0.1352	1.14	0.1844
myristoleate (14:1n5)	0.9	0.6273	1.27	0.0058	1.01	0.8442
pentadecanoate (15:0)	0.91	0.6115	1.15	0.0889	1.08	0.2234
palmitate (16:0)	1.09	0.1966	0.99	0.8799	1.09	0.2606
palmitoleate (16:1n7)	1.02	0.9247	1.07	0.1202	1.14	0.1589
margarate (17:0)	0.91	0.4135	1.39	0.0056	1.06	0.7559
10-heptadecenoate (17:1n7)	0.9	0.1072	1.22	0.0028	1.2	0.117
stearate (18:0)			1.16	0.0535		
oleate (18:1n9)			1.27	0.0002	1.44	0.0366
cis-vaccenate (18:1n7)			0.85	0.0533	1.4	0.028
trans-vaccenate			1.14	0.2159		
stearidonate (18:4n3)	0.8	0.0017	1.52	0.0007		
nonadecanoate (19:0)	1.07	0.6199	1.77	6.64E-05	1.43	0.0289
10-nonadecenoate (19:1n9)	0.89	0.5441	1.47	0.0043	1.38	0.1122
arachidate (20:0) (eicosanoic acid)	1.44	0.0388	2.04	0.0003		
eicosenoate (20:1n9 or 11)	1.37	0.0606	1.31	0.0098	1.58	0.0614
dihomo-linoleate (20:2n6)	0.8	0.1694	1.09	0.5448	1.16	0.4608
mead acid (20:3n9)	0.73	0.0007	0.8	0.0829	0.73	0.032
arachidonate (20:4n6)	0.92	0.3708	1.1	0.2873	1.04	0.8985
Very Long Chain Fatty Acid						
docosadienoate (22:2n6)			0.98	0.9025		
docosatrienoate (22:3n3)			0.63	0.0226		
adrenate (22:4n6)			0.82	0.042	0.84	0.2475
Essential Fatty Acid (EFA)						
linoleate (18:2n6)	0.9	0.1251	1.19	0.0068	1.22	0.115
linolenate [alpha or gamma; (18:3n3 or 6)]	0.85	0.0669	1.36	0.0014	1.02	0.8248
dihomo-linolenate (20:3n3 or n6)	0.91	0.2491	1.14	0.0955	1.23	0.3367
eicosapentaenoate (EPA; 20:5n3)	1.11	0.3505	1.52	0.0049		
Very Long Chain essential fatty acid (VLCEFA)						
docosapentaenoate (n3 DPA; 22:5n3)	0.97	0.679	0.8	0.0046	1.09	0.7234
docosapentaenoate (n6 DPA; 22:5n6)			0.5	0.0139	0.85	0.5165
docosahexaenoate (DHA; 22:6n3)	0.97	0.7028	0.77	0.0058	1.19	0.5613
Fatty acid, monohydroxy						
16-hydroxypalmitate			1.37	0.0018	1.22	0.2438
4-hydroxybutyrate (GHB)	1.29	0.2576				
13-HODE + 9-HODE	1.11	0.3758	1.45	0.0056	1.06	0.6856
Fatty acid, ester						
n-Butyl Oleate			0.97	0.6974		
Fatty acid, dicarboxylate						
2-hydroxyglutarate	0.85	0.2952	1.16	0.396	0.74	0.193
tetradecanedioate	0.97	0.9599	1.31	0.0159		
hexadecanedioate	1.13	0.3547	1.48	0.0002	1.09	0.5434
undecanedioate					1.25	0.4572
azelate (nonanedioate)					1.35	0.5627
Fatty acid, branched						
13-methylmyristic acid	0.95	0.9113	1.27	0.0083	1.13	0.3373
15-methylpalmitate	0.9	0.6245	1.24	0.0144	1.14	0.2941
isopalmitic acid	1	0.8428			1.2	0.4129
17-methylstearate	1.03	0.7998	1.76	0.0003	1.54	0.0354
Eicosanoid						
12-HETE	0.76	0.2593	1.33	0.0839		
Endocannabinoid						
oleic ethanolamide	0.9	0.3134				
palmitoyl ethanolamide			1.24	0.0709	1.01	0.8006
Fatty acid synthesis (BCAA metabolism)						
malonylcarnitine	1.06	0.5318				
propionylcarnitine			1.59	0.034	1.27	0.1192
butyrylglycine			1.16	0.0581		
butyrylcarnitine					0.66	0.224
Carnitine						
deoxycarnitine	0.92	0.7476	1.14	0.3875	1.85	0.0012
carnitine	1.05	0.4964	0.92	0.3327	1.18	0.0056
3-dehydrocarnitine*	1.23	0.137	0.74	0.0267	0.88	0.428
acetylcarnitine	1.17	0.3531	1.14	0.5386	1.1	0.8754
Bile acid metabolism						
cholate	0.7	0.1489	1.88	0.132		
taurocholate	2.8	0.6215	0.87	0.4922	0.55	0.0502
taurochenodeoxycholate	4.18	0.3596	1.43	0.2459		
deoxycholate	0.61	0.0459	2.81	0.001		
taurodeoxycholate	4.12	0.3213	2	0.0057		
tauro(alpha + beta)muricholate	2.17	0.7567				
alpha-muricholate			1.68	0.0124		
Glycerolipid						
choline phosphate	0.85	0.0808	1.1	0.3273	0.98	0.8131
Choline	1.04	0.6797	1.05	0.3846	1.19	0.0375
glycerol 3-phosphate (G3P)	1.08	0.4341	0.81	0.0869	1.14	0.0788
glycerophosphorylcholine (GPC)	1	0.9172	0.53	5.53E-05	1.05	0.8263
ethanolamine	0.93	0.7942	2.11	0.0038		
phosphoethanolamine	0.94	0.4324	1.36	0.2016	0.76	0.1075
glycerol	0.9	0.3289	1.01	0.8031	1.14	0.2035
cytidine 5'-diphosphocholine	1.02	0.7133				

Fig. S3. (Continued)

	BAT	BAT	Liver	Liver	WAT	WAT
	Fold Change	p value	Fold Change	p value	Fold Change	p value
Inositol metabolism						
myo-inositol	0.73	0.0224	1.39	0.0172	0.64	0.0028
inositol 1-phosphate (I1P)	0.84	0.0825	1.09	0.1494	1.14	0.5226
scyllo-inositol	0.61	0.038			0.37	0.0005
Beta oxidation						
3-hydroxybutyrate (BHBA)	3.01	6.23E-05	1.19	0.2014		
acetyl CoA	1.52	0.0491				
Lysolipid						
1-palmitoylglycerophosphoethanolamine	1.06	0.6199	1.06	0.9319	1.33	0.1735
2-palmitoylglycerophosphoethanolamine*	0.98	0.9745	1.08	0.8573		
1-palmitoleoylglycerophosphoethanolamine*	1.15	0.5012	2.15	0.0394	1.35	0.3675
1-heptadecanoylglycerophosphoethanolamine*			1.6	0.2041		
1-stearoylglycerophosphoethanolamine	1.05	0.8242	1.64	0.0174	1.16	0.4105
1-oleoylglycerophosphoethanolamine	0.99	0.8899	1.3	0.2409	2.16	0.0051
2-oleoylglycerophosphoethanolamine*	0.95	0.6983	1.7	0.0504	1.59	0.0637
1-linoleoylglycerophosphoethanolamine*	0.97	0.9461	1.87	0.0167		
2-linoleoylglycerophosphoethanolamine*	0.8	0.5271	4.2	0.0044		
1-arachidonoylglycerophosphoethanolamine*	0.84	0.2999	1.54	0.0081	1.28	0.1487
2-arachidonoylglycerophosphoethanolamine*	0.77	0.3015	1.71	0.0345	1.02	0.8116
2-docosapentaenoylglycerophosphoethanolamine*			1.58	0.3006		
2-docosahexaenoylglycerophosphoethanolamine*	0.8	0.8797	1.93	0.091		
1-myristoylglycerophosphocholine			1.88	0.2317		
1-palmitoylglycerophosphocholine	0.61	0.0745	2.05	0.0524	1.15	0.1641
2-palmitoylglycerophosphocholine*			1.89	0.0715		
1-palmitoleoylglycerophosphocholine*	0.77	0.1093	2.77	0.0186		
2-palmitoleoylglycerophosphocholine*			2.14	0.0849		
1-heptadecanoylglycerophosphocholine			2.64	0.005		
1-stearoylglycerophosphocholine	0.59	0.0328	1.52	0.1495	1.12	0.4389
1-oleoylglycerophosphocholine	0.58	0.2491	2.32	0.0302	1.34	0.0279
2-oleoylglycerophosphocholine*	0.53	0.2038	2.16	0.0162	1.28	0.0637
1-linoleoylglycerophosphocholine	0.74	0.1729	3.08	0.0035	1.13	0.4748
2-linoleoylglycerophosphocholine*	0.89	0.6515	3.15	0.0035		
1-eicosatrienoylglycerophosphocholine*			1.64	0.068		
2-eicosatrienoylglycerophosphocholine*			2.47	0.0022		
1-arachidonoylglycerophosphocholine*	0.74	0.2128	1.85	0.0627		
2-arachidonoylglycerophosphocholine*			2.06	0.0592		
1-docosahexaenoylglycerophosphocholine*			1.6	0.1321		
2-docosahexaenoylglycerophosphocholine*			1.72	0.1191		
1-palmitoylglycerophosphoinositol*	0.92	0.648	1.25	0.1058	0.83	0.2227
1-stearoylglycerophosphoinositol	0.86	0.5801	1.31	0.0402		
2-stearoylglycerophosphoinositol*	0.83	0.3318	1.34	0.0377	1.2	0.5099
1-arachidonoylglycerophosphoinositol*	0.98	0.8734	1.48	0.0031		
2-arachidonoylglycerophosphoinositol*	0.92	0.9453	1.56	0.0038		
1-palmitoylplasmenylethanolamine*	1.08	0.4857	0.93	0.7643	1.38	0.1049
Monoacylglycerol						
1-palmitoylglycerol (1-monopalmitin)			1.13	0.1685		
1-stearoylglycerol (1-monostearin)	0.78	0.1649	1.05	0.6119		
1-oleoylglycerol (1-monoolein)	0.71	0.3015				
2-oleoylglycerol (2-monoolein)	0.59	0.1847				
1-linoleoylglycerol (1-monolinolein)			1.01	0.8671		
Diacylglycerol						
1,2-dipalmitoylglycerol	0.85	0.4606				
Sphingolipid						
sphingosine	0.75	0.3588	2.14	0.0117		
palmitoyl sphingomyelin	0.75	0.1315	1.06	0.3975	1.06	0.498
stearoyl sphingomyelin	0.83	0.1837			1.02	0.9977
sphinganine			1.8	0.0772		
Sterol/Steroid						
cholesterol	0.94	0.6452	1.24	0.0035	1.14	0.298
7-alpha-hydroxycholesterol	0.89	0.5048			0.58	0.1395
7-beta-hydroxycholesterol	0.94	0.7896	0.73	0.1612	0.99	0.9059
squalene			0.9	0.4556		
dihydrocholesterol			1.4	0.0099		
corticosterone	1.33	0.1456				
Tocopherol metabolism						
alpha-tocopherol	0.69	0.0481	1.2	0.0716	0.95	0.7141

Fig. S3. (Continued)

B

Biochemical Name	BAT Fold-change	BAT p value	Liver Fold-change	Liver p value	WAT Fold-change	WAT p value
Fructose, maltose						
Fructose	2.04	0.5686			0.97	0.728
maltose	1.65	0.0874	1.45	0.0142	0.47	0.0274
maltopentaose			0.76	0.0629		
maltohexaose			0.58	0.0223		
Maltotriose	1.44	0.0955	1.11	0.483		
Fructose-6-phosphate	0.88	0.88				
Glycolysis, Gluconeogenesis, pyruvate						
glucose	1.27	0.2848	1.07	0.1999	0.7	0.0575
glucose-6-phosphate (G6P)	0.99	0.8021	0.91	0.718	0.82	0.3339
3-phosphoglycerate	0.88	0.6647	1.29	0.025		
phosphoenolpyruvate (PEP)			1.54	0.1572		
Lactate	1.08	0.5366	1.1	0.0902	0.99	0.9906
fructose 1,6-diphosphate, g	1.78	0.048			0.93	0.517
1,5-anhydroglucitol (1,5-AG)	1.23	0.0444	0.74	0.3075		
Kreb's Cycle						
citrate	1.22	0.1894	1.59	0.2127	0.79	0.4215
succinyl CoA			0.84	0.3182		
fumarate	0.81	0.4141	1.23	0.0626	0.83	0.4579
malate	0.9	0.3567	1.2	0.0413	0.84	0.4608
cis-aconitate	1.2	0.1274			2.35	0.2707
Succinate					0.57	0.0135
succinylcarnitine	1.09	0.4001	1.02	0.9535	2.25	0.0017
propionylcarnitine			1.59	0.034	1.27	0.1192
Oxidative Phosphorylation						
acetylphosphate			1.2	0.0183	1.23	0.1239
phosphate	1.08	0.22	1.19	0.0042	1.1	0.3988
pyrophosphate (PPi)	1.24	0.6115	1.46	0.0247		
Nucleotide sugars, pentose metabolism						
ribitol			1.26	0.0029		
ribose	1	0.8342	1.28	0.0456		
xylitol			1.38	0.0367		
UDP-glucuronate	1.47	0.0016				
Aminosugars metabolism						
erythronate*	0.72	0.0414	1.32	0.1828		
N-acetylneuraminate	1.03	0.6181				
glucosamine			1.06	0.5724		

Fig. S3. (Continued)

Biochemical Name	BAT Fold-change	BAT p value	Liver Fold-change	Liver p value	WAT Fold-change	WAT p value
Glycine, serine and threonine metabolism						
glycine	1.05	0.6007	1.31	0.024	0.86	0.1162
sarcosine (N-Methylglycine)			1.49	0.0033		
dimethylglycine	0.96	0.8582	1.39	0.0417		
N-acetylglycine	1.3	0.0691				
serine	0.95	0.9893	1.4	0.0017	1.02	0.8729
homoserine	0.89	0.6692	1.23	0.4763		
threonine	1.03	0.642	1.25	0.0011	0.87	0.096
betaine	1.4	0.0417	1.27	0.1825		
Alanine and aspartate metabolism						
aspartate	0.96	0.96	1.18	0.2391	0.61	0.0002
asparagine	0.77	0.77	1.11	0.0382	0.81	0.3862
alanine	1.02	0.7058	1.16	0.0629	0.93	0.5214
3-ureidopropionate	1.69	0.0079				
Glutamate metabolism						
glutamate	0.91	0.3279	1.06	0.6568	0.41	0.0002
glutamine	1	0.8907	1.19	0.0142	1	0.9503
gamma-aminobutyrate (GABA)	0.85	0.7982	1.36	0.1592		
N-acetylglutamate	1.07	0.4611	1.33	0.1488		
N-acetylglutamine			1.37	0.0026		
Histidine metabolism						
Histidine	0.96	0.9164	1.12	0.0487	1.05	0.7026
Lysine metabolism						
lysine	1.08	0.9518	1.18	0.0035	0.98	0.7783
2-aminoadipate	1.54	0.0223	1.41	0.0665	1.05	0.7427
pipecolate	1.2	0.2307	1.22	0.0416		
glutaroyl carnitine			1.67	4.32E-05		
Phenylalanine, tyrosine, tryptophan						
phenylalanine	0.93	0.8487	1.29	0.0004	0.99	0.8706
p-cresol sulfate	1.04	0.7212	1.32	0.0296	0.97	0.8429
tyrosine	0.85	0.4261	1.2	0.0656	0.99	0.8517
tryptophan	0.93	0.8457	1.21	0.0167	0.99	0.8631
C-glycosyltryptophan*	0.93	0.9851	1.23	0.007	1.52	0.4213
3-indoxyl sulfate	1.24	0.0571	1	0.9994	1.1	0.6837
Valine, leucine, isoleucine						
isoleucine	0.98	0.9392	1.3	0.0077	0.91	0.4249
leucine	0.93	0.8417	1.27	0.0016	0.99	0.8872
valine	0.95	0.884	1.3	0.0025	0.93	0.4233
isobutyrylcarnitine	0.89	0.5682	0.73	0.0449	1.7	0.0399
2-methylbutyroylcarnitine	1.08	0.5413	0.8	0.2087	1.4	0.0261
Cysteine, methionine, SAM, taurine						
cysteine	0.65	0.0645	1.27	0.0385	0.98	0.8532
S-adenosylhomocysteine (SAH)	0.97	0.9407	1.25	0.0218	1.27	0.141
methionine	0.87	0.2618	1.27	0.0005	1	0.9962
2-hydroxybutyrate (AHB)	2.11	0.0028	1.21	0.4537		
taurine	1.13	0.0073	0.94	0.2942	1.13	0.0401
Urea cycle, arginine, proline						
arginine	1.06	0.3687	1.36	0.0254	0.75	0.0781
ornithine	0.79	0.2674	1.63	0.0309	1.33	0.8332
urea	1.15	0.1964	2.05	0.0002	1.03	0.6378
proline	0.83	0.2911	1.24	0.0009	1.03	0.7976
citrulline	1.15	0.1513	1.15	0.1414	1.21	0.0207
trans-4-hydroxyproline	1.11	0.6161	1.68	0.0159	1.31	0.2034
dimethylarginine (SDMA + ADMA)	0.78	0.2799	1.38	0.0044		
Creatine metabolism						
creatine	1.12	0.506	0.85	0.0317	0.74	0.0003
creatinine	0.99	0.8802	0.97	0.5972		
Polyamine metabolism						
5-methylthioadenosine (MTA)	0.98	0.9386				
putrescine	0.76	0.1721				
spermidine	0.8	0.2051				
Dipeptide						
glycylvaline			1.58	0.0191		
glycylproline			1.57	0.0027		
glycylisoleucine	1.22	0.3116	1.19	0.4216		
glycylleucine	1.05	0.5492	1.54	0.0316		
glycylphenylalanine			1.06	0.877		
prolylglycine			1.46	0.0302		
isoleucylglycine			1.3	0.1607		
serylleucine	1.1	0.4952	1.22	0.0473		
Glutathione metabolism						
glutathione, reduced (GSH)	2.36	0.0225	0.55	0.052	0.68	0.1057
S-methylglutathione			0.66	8.31E-06		
5-oxoproline	0.86	0.186	1.07	0.2239	1.39	0.3097
glutathione, oxidized (GSSG)	0.9	0.417	0.99	0.8248	0.86	0.1216
cysteine-glutathione disulfide	0.51	0.0246	1.23	0.0113	1.14	0.3701
Nicotinate and nicotinamide metabolism						
nicotinamide	1.03	0.7029	1.11	0.0134	1.07	0.6118
nicotinamide adenine dinucleotide (NAD+)	1.19	0.2997	1.26	0.0004		
nicotinamide adenine dinucleotide reduced (NADH)			1.27	0.001		
Riboflavin metabolism						
flavin adenine dinucleotide (FAD)	0.98	0.8591	1.22	7.31E-05	1.14	0.243
riboflavin (Vitamin B2)	0.97	0.9792	1.43	0.0001		
flavin mononucleotide (FMN)			1.39	0.0024		

Fig. S3. (Continued)

C

	BAT Fold Change	BAT p value	Liver Fold Change	Liver p value	WAT Fold Change	WAT p value
Purine metabolism/(hypo)xanthine/inosine						
xanthine	0.95	0.7843	1.04	0.1344	1.11	0.2166
xanthosine	1.01	0.6682	1.76	0.0005		
hypoxanthine	0.96	0.9838	1.25	0.0004	1.38	0.0332
inosine	1.13	0.2063	1.26	0.089	1.26	0.2169
inosine 5'-monophosphate (IMP)	1.23	0.3617			0.81	0.1943
2'-deoxyinosine			1.01	0.9116		
Purine metabolism / adenine containing						
adenine	1.03	0.6121	0.76	0.0145	1.05	0.8785
adenosine	0.96	0.9224	1.15	0.0871	1.73	0.0053
adenosine 2'-monophosphate (2'-AMP)	0.93	0.7402	1.03	0.6592	0.64	0.0048
adenosine 3'-monophosphate (3'-AMP)	0.73	0.3016	1.21	0.0198	0.85	0.5489
adenosine 5'-monophosphate (AMP)	0.82	0.7711	1.16	0.2101	0.67	0.0403
adenosine 5'-diphosphate (ADP)	1.14	0.1917	1			
adenosine-5'-diphosphoglucose	1.02	0.7259				
N1-methyladenosine			1.02	0.8679		
2'-deoxyadenosine 3'-monophosphate			1.05	0.8065		
adenosine 3',5'-diphosphate			1.35	0.1367		
Purine metabolism, guanine containing						
guanosine	1.07	0.5285	0.99	0.891	1.3	0.2408
guanosine 5'- monophosphate (5'-GMP)	1.01	0.802			0.88	0.275
2'-deoxyguanosine			1.13	0.3146		
Purine metabolism/urate						
urate	0.89	0.4263	1.35	0.3478	1.31	0.2745
allantoin	0.87	0.4231	0.99	0.869		
Pyrimidine metabolism/cytidine						
cytidine	0.93	0.7402	1.27	0.0108	0.9	0.2596
cytidine 5'-monophosphate (5'-CMP)	0.99	0.9479			0.94	0.4422
2'-deoxycytidine			1.32	0.0626		
2'-deoxycytidine 5'-monophosphate			1.35	0.1189		
Pyrimidine metabolism/thymine and uracil						
thymidine	1.07	0.5647				
uracil	0.79	0.3416	1.12	0.288	1	0.8891
5,6-dihydrouracil	1.05	0.5542				
uridine	0.95	0.5324	1.21	0.0392	1.31	0.0266
pseudouridine	0.98	0.9355	1.22	0.261	1.61	0.4231
uridine monophosphate (5' or 3')	0.97	0.7753			0.65	0.0085
orotate			1.44	0.0128		
Purine and pyrimidine metabolism						
methylphosphate			1.22	0.0266		
Ascorbate and aldarate metabolism						
ascorbate (Vitamin C)	1.27	0.1407	1.13	0.2121	1.26	0.8915
dehydroascorbate	0.78	0.2512				
gulono-1,4-lactone			1.91	2.97E-06		
arabonate			1.08	0.4614		
Folate metabolism						
5-methyltetrahydrofolate (5MeTHF)	1.18	0.1352	0.67	0.1389		
biopterin			1.23	0.2412		
dihydrobiopterin			1.28	0.1727		
Nicotinate and nicotinamide metabolism						
nicotinamide	1.06	0.5351	1.11	0.0134	1.07	0.6118
nicotinamide adenine dinucleotide (NAD+)	1.14	0.4337	1.26	0.0004		
adenosine 5'diphosphoribose	1.35	0.0337				
nicotinate	1.25	0.0471				
otinamide adenine dinucleotide reduced (NADH)			1.27	0.001		
trigonelline (N'-methylnicotinate)					1	
Pantothenate and CoA metabolism						
pantothenate	1.04	0.6752	1.37	0.0005	1.27	0.0258
phosphopantetheine	1.74	0.0445	0.57	0.283		
acetyl CoA	1.52	0.0491				
3'-dephosphocoenzyme A	2.04	0.029	0.58	0.0551		
coenzyme A	2.69	0.0059	0.64	0.1068		
Riboflavin metabolism						
flavin adenine dinucleotide (FAD)	0.97	0.8778	1.22	7.31E-05	1.14	0.243
riboflavin (Vitamin B2)	1	0.8289	1.43	0.0001		
flavin mononucleotide (FMN)			1.39	0.0024		
Thiamine metabolism						
thiamin diphosphate	1.2	0.2047				
thiamin (Vitamin B1)			1.12	0.1002		
Tocopherol metabolism						
alpha-tocopherol	0.69	0.0481	1.2	0.0716	0.95	0.7141
Vitamin B6 metabolism						
pyridoxate	1.09	0.5451	1.59	0.0583	0.32	0.6505

Fig. S3. Heat map of metabolites from BAT, liver, and WAT of control and treated animals showing fold-change (treated/control) and *P* values. (*A*) Lipid metabolism, (*B*) carbohydrate metabolism, (*C*) protein and vitamin metabolism. Red: increased, $P < 0.05$; pink: increased, $P < 0.1$; green: decreased, $P < 0.05$, light green: decreased, $P < 0.1$.

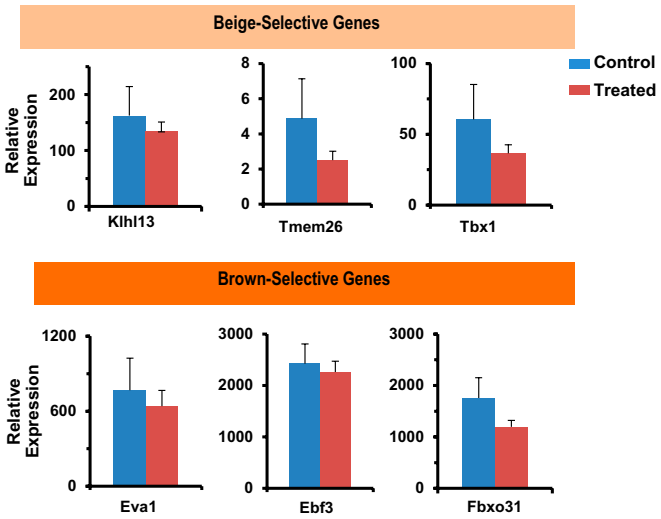

Fig. S4. mRNA levels in interscapular BAT genes specific to beige or brown adipocytes in control (blue bars) and ShK-186–treated mice (brown bars).

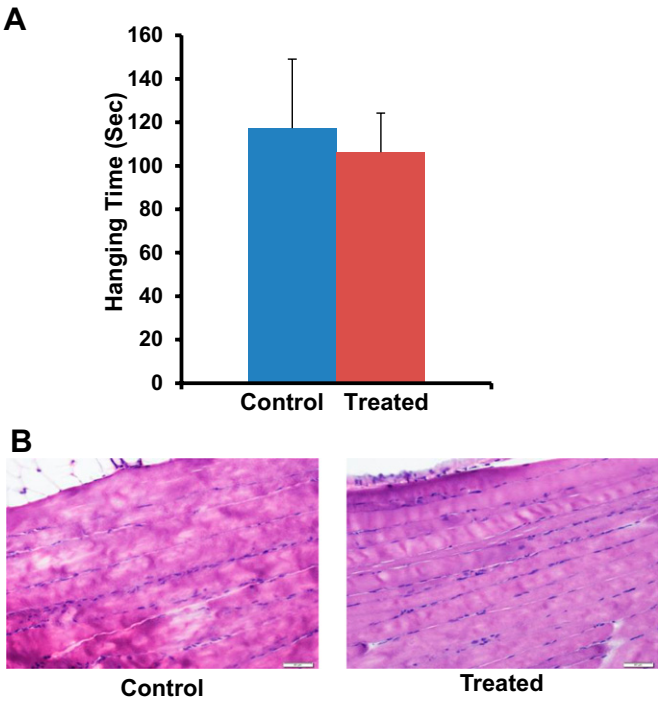

Fig. S5. (*A*) Hanging test shows normal muscle strength in control and treated mice. (*B*) Histological analysis shows that skeletal muscle in treated mice is no different from that in controls. Together, these data suggest that the increased protein utilization in the livers of ShK-186–treated mice is not due to protein catabolism in skeletal muscle.

Table S1. Comparison of ShK-186 therapy and Kv1.3 gene deletion on diet-induced obesity

Parameter	Kv1.3 KO (10) diet Bio-Serv F3282 measured at 8 mo of age	Kv1.3 KO (5, 6) diet D12266B condensed milk measured at 9.5 mo of age	ShK-186 diet TD.88137 + fructose measured at 4.5 mo of age
Weight	Decreased	Decreased	Decreased
Leptin	Decreased	Decreased	Decreased
Adiposity	Not reported	Decreased	Decreased
Blood sugar	Decreased	Decreased	Decreased
HbA1C	Not reported	Not reported	Decreased
Cholesterol, LDL	Not reported	Not reported	Decreased
Insulin	Decreased	Decreased	Decreased
Peripheral insulin sensitivity	Increased	Not reported	Increased
^{18}F-FDG uptake by BAT	Not reported	Not reported	Increased
Brown fat metabolic activity	Not reported	Not reported	Increased
Total energy expenditure	Increased	Increased	Increased
Light-phase energy expenditure	Not reported	Increased	Increased
Liver metabolism	Not reported	Not reported	Increased
Locomotor activity	Unchanged	Unchanged	Unchanged

Despite the use of three different diets, and differences in the age when measurements were made, the effects of ShK-186 therapy and Kv1.3 gene deletion are remarkably similar. These data strongly suggest that the antiobesity activities of ShK-186 are predominantly due to pharmacological actions on Kv1.3.

Table S2. Composition of obesity diet: TD.88137 (solid), 60% fructose/water (wt/vol; fluid)

Diet components	TD.88137 components, % by weight	TD.88137, % by weight	TD.88137, % kcal	TD.88137 + 60% fructose/water, % kcal
Protein	DL-methionine 0.3, casein 17, total = 17.3	17.3	15.2	~11
Carbohydrate	Sucrose 34.55, corn starch 13.95, total = 48.5	48.5	42.7	~58
Fat	Anhydrous milk fat 21, casein 0.2, total = 21.2	21.2	42	~31
Mineral mix	3.5	3.5		
Cellulose	5.0	5.0		
Vitamin mix	1.0	1.0		

The percentage of kilocalories from carbohydrate, fat, and protein for the combined obesity diet (TD.88137 + fructose/water) was determined as follows. Mice consumed roughly 1.5–2 g/d of Teklad TD.88137 and 0.6–2 mL/d (0.36–1.2 g fructose) of 60% fructose/water. Assuming a daily consumption of 2 g food and 1.5 mL 60% fructose/water, mice on the combination diet consumed protein 0.346 g, carbohydrate from food and fluid 1.87 g (0.97 + 0.9), and fat 0.424 g (total = 2.64 g). The total calorie consumption per day = protein 1.384 kcal, carbohydrate 7.48 kcal, 3.816 kcal = total 12.68 kcal/d (assuming 4 kcal/g for carbohydrate and protein, 9 kcal/g for fat). Calorie contributions in percentage terms would equal: protein 10.91%, carbohydrate 58.99%, 30.1% fat.

Table S3. Comparison of diets used in our study (Teklad 7001 chow, TD.88137 + 60% fructose) with chow and obesity diets used in Kv1.3$^{-/-}$ mice

Diet components	Chow Teklad 7001 4% fat, % kcal	Chow (7, 8) Purina 5001, % kcal	Obesity diet TD.88137 + 60% fructose/water, % kcal	Obesity diet (7, 8) D12266B condensed-milk diet, % kcal	Obesity diet (9) Bio-Serv F3282, % kcal
Protein	34	28.5	~11	16	14.9
Carbohydrate	53	58.0	~58	51	26.0
Fat	13	13.5	~31	32	59.0

Our combined diet has similar calorie contributions to the D12266B condensed-milk diet, with the difference that a significant fraction of carbohydrate calories in our obesity diet comes from fructose.

Table S4. Energy expenditure in control and treated (ShK-186 500 μg/kg) mice on the obesity diet during the light/dark phase and over 24 h

Mice	Dark-phase EE, kcal/12 h	Light-phase EE, kcal/12 h	Daily EE, kcal/24 h
Control	7.91 ± 0.39	6.63 ± 0.31	14.55 ± 0.70
Treated	9.23 ± 0.34	8.19 ± 0.29	17.42 ± 0.62

Table S5. Food intake in grams in control and treated (ShK-186 500 μg/kg) mice on the obesity diet during the light/dark phase and over 24 h

Mice	Dark-phase food, g/12 h	Light-phase food, g/12 h	Daily food, g/24 h
Control	1.81 ± 0.1	0.45 ± 0.05	2.26 ± 0.08
Treated	1.44 ± 0.15	0.75 ± 0.11	2.19 ± 0.24

Table S6. Fructose intake in grams from fructose/water in control and treated (ShK-186, 500 μg/kg) mice on the obesity diet during the light/dark phase and over 24 h

Mice	Dark-phase drink, g/12 h	Light-phase drink, g/12 h	Daily drink, g/24 h
Control	0.5 ± 0.03	0.24 ± 0.04	0.63 ± 0.04
Treated	0.65 ± 0.04	0.39 ± 0.05	1.04 ± 0.08

Fructose (g) was calculated by the formula: milliliters of fructose/water consumed × fructose concentration (wt/vol). The kilocalories were calculated by multiplying fructose (g) consumed × 4 mL of fructose/water consumed × fructose concentration (wt/vol) × 4 = kilocalories.

Table S7. Calorie intake in control and treated (ShK-186, 500 μg/kg) mice on the obesity diet over 24 h

Calorie intake	Control	Treated
Food, g/24 h	2.26 ± 0.08	2.19 ± 0.24
Carbohydrates from food, g/24 h	1.1 ± 0.04	1.06 ± 0.12
Carbohydrates from fructose, g/24 h	0.63 ± 0.04	1.04 ± 0.08
Total carbohydrates, g/24 h	1.72 ± 0.04	2.1 ± 0.15
Protein, g/24 h	0.39 ± 0.01	0.38 ± 0.04
Fat, g/24 h	0.48 ± 0.02	0.47 ± 0.05
Carbohydrates calories, kcal/24 h	6.89 ± 0.18	8.41 ± 0.61
Protein calories, kcal/24 h	1.56 ± 0.06	1.52 ± 0.17
Fat calories, kcal/24 h	4.31 ± 0.15	4.18 ± 0.46
Total calories	12.77 ± 0.34	14.11 ± 1.19 ($P = 0.29$)

Carbohydrate and protein: 4 kcal/g; fat: 9 kcal/g.

Table S8. Quantification of Kv1.3 protein expression in BAT

Diet	Mouse	Kv1.3, 80 KDa	Kv1.3, 60 KDa	Kv1.3 total	Actin	Kv1.3 total/actin
Chow	1	1,708	1,933	3,642	26,049	0.14
Obesity	2	1,128	1,523	2,651	23,844	0.11

Table S9. Quantification of Kv1.3 protein expression in liver

Diet	Mouse	Kv1.3, 80 KDa	Kv1.3, 60 KDa	Kv1.3 total	Actin	80 KDa Kv1.3/actin, average	60 KDa Kv1.3/actin, average	Kv1.3 total/actin, average
Chow	1	0.00094	0.00018	0.0011	0.0032			
	2	0.00121	0.00022	0.0014	0.0024	0.4018	0.0751	0.4769
Obesity	3	0.00241	0.00064	0.0030	0.0024			
	4	0.00420	0.00111	0.0053	0.0030	1.1967	0.3167	1.5134